Flat-structural Motives in Small Alumino−Carbon Clusters C_nAl_m ($n = 2-3$, $m = 2-8$)

Fedor Y. Naumkin*

Faculty of Science, University of Ontario Institute of Technology, Oshawa, ON L1H 7K4, Canada

Received: November 27, 2007; Revised Manuscript Received: February 17, 2008

Small clusters consisting of a carbon diatom or triatom and several aluminum atoms are investigated ab initio, at an MP2 level of theory. The mainly ionic character of C−Al bonding predominantly leads to structures different from corresponding hydrocarbons (also if starting from analogous initial geometries), while still producing closed-shell ground states. It is found that in many cases stable geometries correspond to flat CAl_3 units. These include unique metal-framed dicarbon and tricarbon all-flat species with unusual planar tetra-coordination. Another frequent feature is a hyper-coordination of carbon atoms, supported by their high negative charges and critically examined via atom-in-molecule calculations. Also characterized are anionic states, electronic excitation and ionization, electron attachment and detachment, and charge distributions.

Introduction

Metal clusters have specific geometries and physical-chemical properties determined by their quantum sizes and large surface-to-volume ratio. These properties also depend on the cluster shape and composition and vary upon doping with other metal or nonmetal atoms. Doping with molecular species adds further multidimensionality to the cluster structure and property variations, which can be useful for practical applications such as catalysis, new (nanostructured) materials, or molecular devices. This work focuses on molecules incorporated into metal clusters up to being their cores, rather than adsorbed on their surfaces. Recent examples of such systems include Si_3Au_3 and Au_3BO^- complexes[1,2] (also considered from the viewpoint of metal−carbon versus hydrogen−carbon bonding) and a gold-cage cluster with a molecular carbon core, C_5Au_{12}[3] (a structural analogue of C_5H_{12}). In the present work, analogous smaller systems are investigated, namely, diatomic and triatomic carbon molecules with up to eight aluminum atoms attached.

Previous studies have dealt with C_2Al and C_2Al_2 species.[4,5] It was found that the latter, in its most stable isomer, resembles Al-substituted acetylene, whereas the former is most stable in a T-shaped (or cyclic) geometry, thus without a hydrocarbon analogue. Apparent questions are whether larger similar systems, C_nAl_m, may also have hydrocarbon-like geometries and/or what different structures may be found. One such system is C_2Al_3, found[6] to resemble C_2Al_2 with the third aluminum attached on the side (like in C_2Al), thus having no hydrocarbon counterpart.

Related questions are whether C_nAl_m ($n > 1$, $m > 1$) other than C_2Al_2 may have flat geometries, similar to CAl_3[7] and (near-flat) C_2Al_3[6] and/or may perhaps exhibit hyper-coordinated carbon atoms, by analogy to electronically similar carboranes, C_nB_m.[8] In particular, CAl_4 (i.e., Al-substituted methane) has previously been found to have both flat and tetrahedral isomers, the latter being more stable,[9] and CAl_4^- is predicted to be flat.[10] These flat systems have unusual planar tetra-coordination of carbon. It is therefore interesting to check if such a feature may also be present in larger alumino-carbon clusters and also how the extra charge influences shapes of their anions. The present study is aimed to address the issues mentioned above.

* E-mail: fedor.naumkin@uoit.ca.

Computational Tools and Methods. Calculations have been carried out at the MP2 level with the aug-cc-pvtz and cc-pvtz basis sets[11] for carbon and aluminum, respectively, as implemented in the NWChem ab initio package.[12] Auxiliary calculations have been carried out at the DFT level with the PBE0 functional and the same basis sets.

At the MP2 level, the C_2 and Al_2 equilibrium internuclear distances are calculated as $R_e = 1.25$ and 2.45 Å, respectively, reproducing experimental data[13] within 0.01 Å. The predicted dissociation energy $D_e = 1.39$ eV for Al_2 fits well the experimental values 1.61 eV (listed in the NIST database[13]) and 1.36 eV (as cited in ref 14). For CAl, values $R_e = 1.97$ Å and $D_e = 3.51$ eV are calculated, favorably comparing with values of 1.95 Å from experiments[15] and 1.95 Å and 3.41 eV from CCSD(T) calculations.[16] The electron affinity of C_2 and ionization potential of Al are predicted to be 3.26 and 5.81 eV, respectively, which are in a nice agreement with experimental values of 3.27 and 5.99 eV.[13]

For each C_nAl_m system, all-atom optimization has been performed in a low symmetry (C_1), and energy minima have been verified by vibrational frequency calculations. Charge distributions have been characterized in terms of natural charges on atoms. Atom-in-molecule (AIM)[17] calculations have been employed to analyze critical points and electron densities. The obtained geometries have been visualized using the ViewMol3D software,[18] and the electron densities were plotted with the Molekel software.[19]

Because the dissociation energies decrease in the row C−C, C−Al, Al−Al, in the present study the initial geometries of C_nAl_m have been limited to nondissociated dicarbon or tricarbon in contact with aluminum atoms. In particular, geometries analogous to those of hydrocarbon counterparts (with the same number of hydrogens), facilitating efficient C−Al bonding, have been employed. Only even numbers of Al atoms (beyond $m = 1$) have been chosen, sufficient to complement the system to a closed shell. The relative stabilization of the obtained singlet states have been checked by comparing with the triplet states of the systems. Although the present study is not aimed at an extensive search of various isomers of each C_nAl_m, the above cluster-construction logic is expected to lead to, at least, low-energy local minima.

10.1021/jp711230x CCC: $40.75
Published on Web 04/22/2008

TABLE 1: Equilibrium Parameters (in eV and Å) of C_nAl_m and $C_nAl_m^-$ Clusters

system		symmetry/state	D_e[a]	R_e(C−C)	R_e(C−Al)	R_e(Al−Al)
C_2Al	linear	$C_{\infty v}/^2\Sigma$	4.10 and 4.68[c]	1.19, 1.25[c]	1.98, 2.02[c]	
	T-shaped	$C_{2v}/^2A_1$	5.51 and 5.06[c]	1.28, 1.29[c]	1.90, 1.94[c]	
C_2Al_2	linear	$D_{\infty h}/^1\Sigma_g$	9.99 and 8.60	1.25, 1.25[d]	1.97, 1.98[d]	
	T-shaped	$C_{2v}/^1A_1$	7.75 and 6.36	1.28	1.91	2.79
$C_2Al_2^-$	linear		7.3	1.26, 1.27[d]	1.92, 1.94|1.93[d]	
	T-shaped	$C_{2v}/^2B_1$	6.0	1.28	1.97	2.70
C_2Al_4	flat	$D_{2h}/^1A_g$	15.45 and 9.05	1.32	1.98, 2.13[b]	3.33
	side-on	$C_s/^1A'$	14.67 and 8.27	1.30	1.97, 2.10−2.17[b]	2.46−3.04
$C_2Al_4^-$	flat	$D_{2h}/^2B_{2g}$	14.06	1.36	1.91, 2.07[b]	3.24
C_2Al_6	end-on	$C_s/^1A'$	22.84 and 9.18	1.41	1.93, 2.03−2.26[b]	2.61−3.10
	side-on	$C_2/^1A$	22.38 and 8.73	1.35	1.98, 2.11−2.32[b]	2.55−2.88
$C_2Al_6^-$	end-on	$C_s/^2A'$	20.81	1.43	1.96, 2.04−2.58[b]	2.54−2.95
	bipyramid	$D_{4h}/^2B_{1g}$	21.04	1.39	1.91, 2.17[b]	2.91, 3.32
C_3Al_4		$C_{2v}/^1A_1$	14.84 and 8.45	1.32	1.94, 2.15, 2.28[b]	2.94, 3.42
$C_3Al_4^-$		$C_{2v}/^2A_1$		1.31	1.93, 2.19−2.27[b]	2.60, 2.91
C_3Al_6	flat	$D_{2h}/^1A_g$	20.59 and 6.94	1.33	1.99, 2.06, 2.53[b]	2.76, 2.96
	C_3-cycle	$C_2/^1A$	20.67 and 7.01	1.42, 2 × 1.55	2.03−2.28[b]	2.87−3.29
C_3Al_8	convex C_3	$C_s/^1A'$	27.24	1.35−1.36	2.00, 2.07−2.73[b]	2.69−3.09
	concave C_3	$C_{2v}/^1A_1$	27.58	1.42	2.13, 2.19−2.40[b]	2.63−2.75

[a] $C_nAl_m \rightarrow C_n + m$Al and $\rightarrow C_n + Al_m$. [b] For Al on the sides of C_n. [c] See reference 4, CCSD-T/6−311+G*. [d] See reference 5, CCSD-T/6−311+G* | MP2/6−311+G*.

TABLE 2: Vertical Electronic-perturbation Energies (in eV) of C_nAl_m Clusters

system		VIE	VEA	VE* (S=0→1)
C_2Al_2	linear	8.72	0.36	2.33
	T-shaped	8.20	1.60	1.27
C_2Al_4	flat	8.22	1.73	1.77
	side-on	7.71	1.51	1.67
C_2Al_6	end-on	9.54	1.14	3.47
	side-on	7.86	1.07	2.26
C_3Al_4		9.29	1.49	3.21
C_3Al_6	flat	7.07	1.23	1.95
	C_3-cycle	8.15	1.20	2.19
C_3Al_8	convex C_3	8.28	1.44	2.22
	concave C_3	8.12	1.34	2.14

Results and Discussion

C_2Al. Adding a single Al atom to the C_2 molecule can produce a linear isomer (similar to the C_2H radical) or a T-shaped isosceles-triangular isomer (with no hydrocarbon analogue). The latter isomer is more stable by 1.4 eV, which could formally be associated with two C−Al interactions at 0.1 Å shorter distances, compensating for a weaker, 0.1 Å longer C−C bond (Table 1). This is in general accord with previous results[4] (whose parameters are given in Table 1 as well), except for their assignment of the linear geometry as a saddle point at the CCSD-T level. The appreciable lowest vibrational frequency of 480 cm^{-1} in the present MP2 calculations allows us to consider the linear isomer.

From comparison with the C−C bond lengths in isolated C_2 and C_3, the linear and T-shaped C_2Al isomers match triple and double C−C bond pattern, respectively. The two isomers can be used as basic C_2Al units for building and interpretation of larger clusters.

The C_2 unit and Al atoms are negatively and positively charged, respectively, as expected. This supports the higher stability of the T-shaped isomer in terms of Al approaching more closely the negative charge concentrated at the center of C_2. In the linear isomer, the carbon remote from aluminum is slightly positive (Table 3), and the dipole moment is rather small (under

TABLE 3: Natural Charges and Dipole Moments (in e and Debye) of C_nAl_m and $C_nAl_m^-$

system		q(C)	q(Al)	D
C_2Al	linear	0.26, −1.06	0.80	−0.87
	T-shaped	−0.59	1.18	4.68
C_2Al_2	linear	−0.75	0.75	0.0
	T-shaped	−0.52	0.88, 0.16	7.87
$C_2Al_2^-$	linear	−0.83	0.33	
	T-shaped	−0.66	0.62, −0.30	
C_2Al_4	flat	−1.45	0.75, 0.70[a]	0.0
	side-on	−1.34, −0.98	2 × 0.60, {0.42, 0.70}[a]	2.49
$C_2Al_4^-$	flat	−1.65	0.48, 0.67 [a]	
C_2Al_6	end-on	−2.24, −1.44	0.50−0.70	0.28
	side-on	−1.66	2 × 0.30, 4 × 0.68 [a]	0.35
$C_2Al_6^-$	end-on	−2.18, −1.49	0.38−0.58	
	bipyramid	−2.09	2 × 0.67, 4 × 0.46[a]	
C_3Al_4		2 × −1.44, −0.32	0.80	0.78
$C_3Al_4^-$		2 × −1.24, −0.35	0.51, 0.40[a]	
C_3Al_6	flat	2 × −1.80, −0.14	0.59, 0.64[a]	0.0
	C_3-cycle	2 × −1.41, −1.64	4 × 0.77, 2 × 0.69	0.47
C_3Al_8	convex C_3	−1.69, −0.90, −1.90	0.64−0.68, 0.43−0.60[a]	1.18
	concave C_3	2 × −1.74, −0.81	4 × 0.40, {2 × 0.64, 2 × 0.69}[a]	1.83

[a] For Al on the sides of C_n.

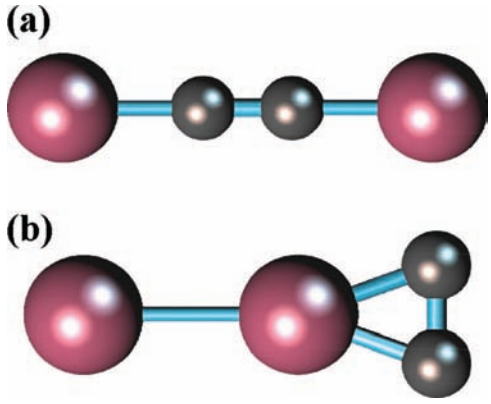

Figure 1. Optimized geometries of linear (a) and T-shaped C_2Al_2 (b).

1 D). The dipole is, however, considerable for the T-shaped isomer, due to a larger charge separation.

C_2Al_2. The C_2Al_2 system with each Al forming a T-shaped unit with C_2 is, however, unstable to isomerization, leading to a linear symmetric AlCCAl structure resembling acetylene with hydrogens replaced by aluminum atoms (Figure 1a). This is consistent with earlier predictions[5] that, however, indicate a minor deviation from linearity (recovered by vibrational averaging). The present result is obtained for the initial geometries either rhombic (with two Al atoms on the opposite sides of C_2) or asymmetric tetrahedral-like (with two diatoms approaching perpendicular to each other and to the axis connecting their centers). The same structure is also obtained when starting from one atom in the linear and one in the T-shaped arrangement or from the CCH_2-like geometry with both Al atoms at one end of C_2 (previously assigned[5] as a saddle point as well). This is consistent with the repulsion of positive aluminum atoms being minimized in linear AlCCAl. In this geometry, the carbon diatom is slightly stretched (by 0.06 Å) relative to linear CCAl and recovers the length of isolated C_2, whereas the C−Al distance is almost unchanged relative to that in C_2Al (Table 1).

Another T-shaped isomer with both Al atoms on the same side of C_2 (Figure 1b) is complementary to previous studies and is significantly higher in energy (by 2 eV). The T-shaped C_2Al "core" of this structure is essentially unperturbed by the second aluminum (Table 1). Both C_2 and Al_2 components of this carbon−metal molecular junction are slightly stretched, relative to isolated diatoms, when in contact with one another. The junction is 6 eV stable to dissociation into the diatoms, whereas it takes only 2 eV (close to the Al_2 dissociation energy) to remove the outer Al atom. Both isomers are obtained in DFT(PBE0) calculations as well, with a 0.3 eV narrower energy gap and with the atom-atom distances and dissociation energies within 0.05 Å and 0.8 eV of the MP2 values.

The linear C_2Al_2 isomer has the lowest electron affinity (under 1 eV) among the systems studied here. The T-shaped isomer is significantly more electronegative (by 1 eV in EA) and has 0.5 eV lower ionization energy and 1 eV lower singlet−triplet gap (Table 2).

The natural-charge distribution indicates negative C and positive Al atoms in both isomers, in the T-shaped isomer the carbons carry somewhat lower charges and the remote aluminum is only slightly charged (Table 3). The latter isomer has a large dipole moment, with the maximum value among the systems studied in this work. It significantly exceeds the value for the T-shaped C_2Al, even though the charges on carbons and the neighboring aluminum are lower, the difference being due to the remote Al atom.

TABLE 4: Electron Densities (in au) at AIM Critical Points of C_nAl_m and $C_nAl_m^-$

system		ρ_c (C−C)	ρ_c (C−Al)
CAl			0.063
C_2Al_2	linear	0.392	0.070
C_2H_2		0.376	0.285
C_2Al_4	flat	0.338	0.061
	side-on	0.357	0.064, 2 × 0.049
C_2Al_6	end-on	0.282	0.065, 0.049−0.054[a]
	side-on	0.319	0.059, 0.044−0.047[a]
$C_2Al_6^-$	bipyramid	0.286	0.066
C_3Al_4		0.327	0.067
C_3Al_6	flat	0.317	0.056, 0.055[a]
	C_3-cycle	0.272, 2 × 0.207	0.052−0.057, 0.040[b]
C_3Al_8	concave C_3	0.276	0.051, 0.039−0.043[a]

[a] For Al on the sides of C_n. [b] For Al above and under C_3 plane.

For the linear isomer the AIM calculations shows axial critical points between C and Al (closer to the aluminum atoms), with the electron density at 17% of the value in the center of the C_2 unit (another critical point) and 10% higher than in isolated CAl (Table 4). By comparison, in C_2H_2 the critical electron density for the C−C bond is about the same as in C_2Al_2, and for the C−H bond it is 70% of this value. This allows for consideration of a C−Al bonding with some covalent (1/4 relative to C−H bonding in C_2H_2) and strong ionic character in C_2Al_2, and the terms "bond" and "bonding" are used for the C−Al interaction in C_nAl_m in such a sense hereafter.

The anions preserve the shapes of their respective neutral counterparts, their stability to dissociation significantly reducing as compared to the neutral systems (more so for the linear isomer). The C−C bond slightly stretches or remains the same, and C−Al shortens or stretches in the linear and T-shaped isomers, respectively, with the Al−Al distance decreasing in the latter (Table 1). The vertical electron-detachment energy is 0.62 eV for linear and 1.59 eV for T-shaped $C_2Al_2^-$, to be compared, for the linear case, with 0.65 eV calculated at the CCSD(T) level and 0.71 eV experimental.[5]

The extra negative charge in the anion goes predominantly to the Al atoms (70−80%), in the T-shaped isomer most of the charge resides on the remote atom (Table 3). This is an apparent result of the charge distribution in the neutral system, with positive aluminum atoms attracting and negative carbons repelling the additional electron.

C_2Al_4. The C_2Al_4 system is formed by adding two Al atoms on the opposite sides of C_2Al_2 (to make T-shaped C_2Al units) and was found to have a stable rhombic structure with the aluminum atoms framing the dicarbon (Figure 2a). This structure could also be seen as being generated by adding another aluminum sideways to C_2Al_3.[6] The flat geometry of C_2Al_4 formally correlates to two (flat) CAl_3 units with common Al atoms and is unlike the tetrahedral shape of the (lowest-energy) CAl_4 counterpart.[9] Both carbons exhibit unusual planar tetracoordination. Alternatively, the system can be viewed as a resonant structure composed of two CAl_2 units with tricoordinated carbons.

Addition of two aluminum atoms to AlCCAl stretches the carbon diatom (by 0.07 Å), similar to making T-shaped C_2Al from C_2, and almost preserves the axial C−Al separations, whereas the new (side) Al atoms are significantly farther (by 0.15 Å) from carbons. Insertion of C_2 into the center of (originally rhombic) Al_4 thus generally preserves its shape, but "inflates" it, with the Al−Al distances becoming considerably longer (by up to 0.8 Å). The DFT(PBE0) calculations with the same basis sets reproduce this equilibrium geometry within

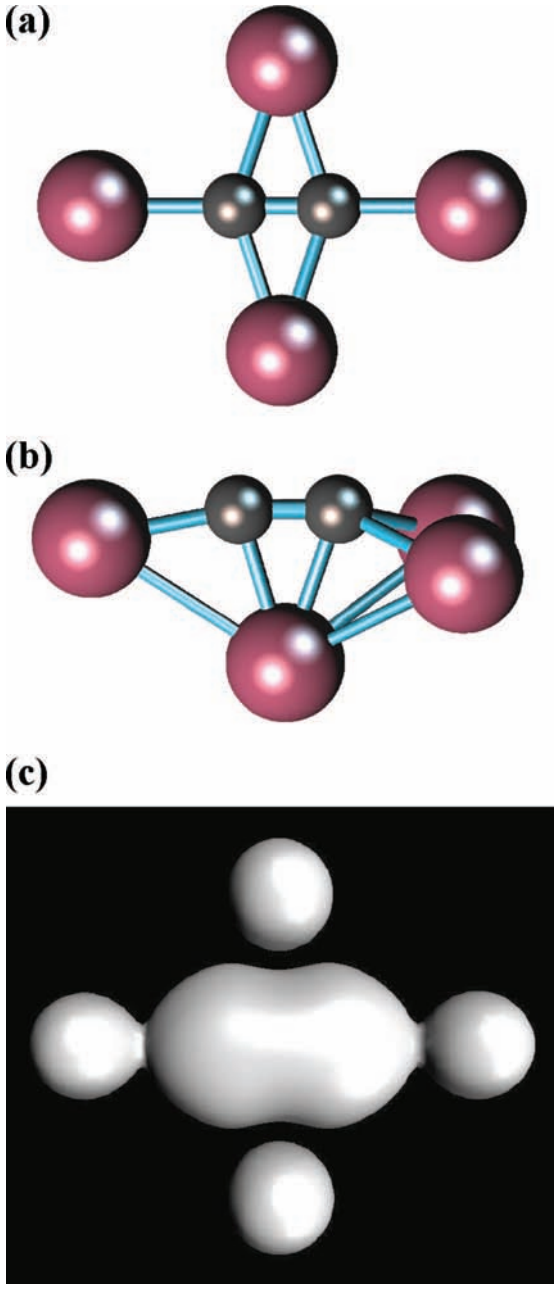

Figure 2. Optimized geometries of planar (a) and side-on C_2Al_4 (b), and calculated electron-density in the planar isomer (c).

0.007 Å in any atom-atom distance and reproduce the dissociation energy within 0.25 eV.

The binding energy of the system is, on average, about 3.9 eV per Al atom, the side aluminum atoms being bound half as weakly as the axial ones (Table 1). The latter is confirmed by the calculated electron-density distribution with a larger density along the axis (Figure 2c), and is consistent with a weaker binding of side Al in the C_2Al_3 species.[6] The AIM critical electron densities for the C−C and axial C−Al bonding are slightly lower than in C_2Al_2 (Table 4).

Another, "side-on" isomer of C_2Al_4 has C_2 attached sideways to a distorted Al_4 cluster (Figure 2b). In particular, this geometry is produced when starting from an ethylene-like hydrocarbon counterpart. This structure can also be obtained by adding two aluminum atoms on the same side of AlCCAl, and it is 0.8 eV higher in energy relative to the rhombic one. The C−C and C−Al distances are about the same as in the flat isomer, whereas the Al−Al distances are significantly shorter (Table 1). The high C_2−Al_4 binding energy (8 eV relative to separated dicarbon and rhombic Al_4) makes it a strong molecular junction, stable by 4 eV to detachment of Al_2. At the DFT(PBE0) level, such an isomer is asymmetric (twisted), with the C_s structure being a low-energy transition state between two equivalent equilibrium geometries, and is 0.6 eV above the rhombic one.

The ionization energy of C_2Al_4 (with 20 valence electrons) is lower than that of C_2Al_2 (Table 2), the value being 0.5 eV higher for the rhombic than for the side-on isomer. Such species (composed of atoms with very different electronegativities) may thus be inaccurately described by the jellium model. The electron affinities are close for both isomers of C_2Al_4 and significantly exceed that of linear C_2Al_2. The corresponding triplet state is 1.55 eV higher in energy in its reoptimized geometry, with the system folding around the AlCCAl axis to the angle of 116 ° and the side C−Al separations increasing by 0.08 Å (the C−C and axial C−Al separations remaining same).

The natural charges on Al atoms in the (ground state) planar isomer are only slightly lower than in C_2Al_2; hence, the C atoms are almost twice as negative (Table 3). In the side-on isomer, the carbon and aluminum charges vary, the C atom with more Al neighbors being more positive. The latter system has a moderate dipole moment.

The anion preserves the flat-rhombic geometry of the neutral system, with the C−C bonds slightly stretched and the C−Al and Al−Al separations shortened (Table 1). This can be considered as a dicarbon-based analogue of (flat) square CAl_4^-.[10] The anion geometry with central C_2 perpendicular to the Al_4 square is a transition state between two equivalent flat-rhombic geometries. The dissociation energy is smaller than for the neutral system. It is interesting to note that the side Al atoms are bound as strongly (by about 7 eV per pair) as the axial ones, unlike in the neutral system (see above).

The adiabatic electron affinity of C_2Al_4 is calculated as 1.88 eV, and the vertical electron-detachment energy of $C_2Al_4^-$ is 2.0 eV. In the anion, the extra negative charge is shared by dicarbon and (mainly) two aluminum atoms along its axis (Table 3).

C_2Al_6. Adding two more Al atoms to rhombic C_2Al_4 results in a "side-on" structure (Figure 3a) with C_2 embedded into the surface of the Al_6 cluster (elongated by the interaction with dicarbon). The geometry can be described as distorted (and slightly concave) C_2Al_4 with both other Al atoms under (or above) its plane, and is also obtained when starting from one additional Al above and one under the C_2Al_4 plane (thus with four aluminum atoms around the C_2 axis). The C−C bond is further (slightly) stretched by adding two more Al atoms to C_2Al_4, their combined attachment energy being 7 eV (Table 1). The C_2−Al_6 binding energy is, however, increased by 0.5 eV relative to C_2−Al_4 (for the corresponding "side-on" isomer), and is almost unchanged per atom.

The dicarbon in C_2Al_6 carries a higher negative charge than in C_2Al_4 due to the larger number of Al atoms donating electron density. The extra electrons support penta-coordinated carbons (Figure 3a). The added aluminum atoms are less positive (Table 3).

The AIM calculations exhibit slightly lower critical electron densities for the C−C and axial C−Al bonding as compared to planar C_2Al_4 (Table 4). Other critical points are found between each C and the two nearest Al atoms (side one from the Al_4 frame and one of two added), with electron densities about three fourths of the value for the axial C−Al pair. This undermines hyper-valence of the formally penta-coordinated carbons.

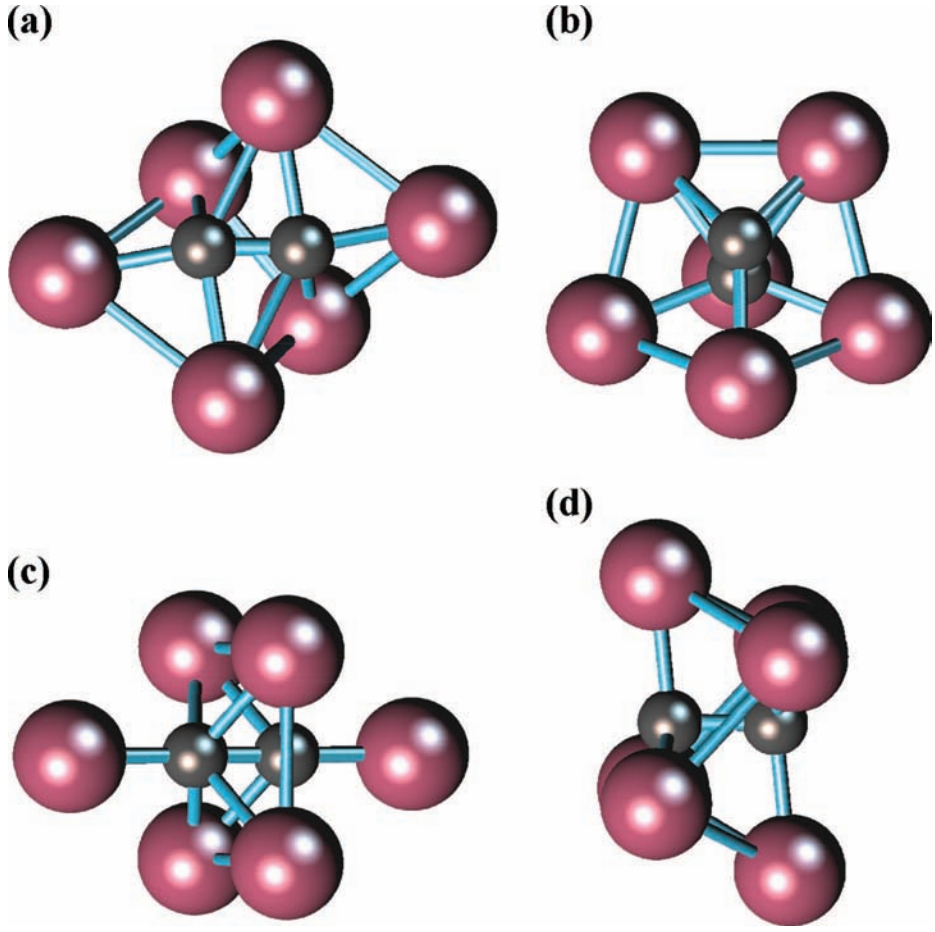

Figure 3. Optimized geometries of side-on (a) and end-on C_2Al_6 (b), the side-on-isomer originated anion (c), and the end-on-isomer related transition state (d).

In the anionic system, the linear AlCCAl unit has a square Al_4 "belt" around its waist, thus forming a symmetric square bipyramid (Figure 3c). Thus, the system switches to this geometry from the "side-on" one when negatively charged and switches back (see above) when the anion is discharged. The C_2 core slightly stretches and the axial C−Al separations shorten in the anion, the Al−Al distances increasing by about 0.4 Å (Table 1). The vertical electron-detachment energy of $C_2Al_6^-$ is calculated to be 3.5 eV, a high value indicating a pretty stable anion, and the adiabatic electron affinity of C_2Al_6 is 1.93 eV. The significant difference between these two values reflects the considerable geometry variation upon charging.

The extra charge in the anion is localized predominantly on the dicarbon (Table 3). Two additional electrons on each carbon atom can promote its hexa-coordination (Figure 3c). The charge on the Al atoms is significantly redistributed in the anion, with each axial aluminum atom becoming more positive than those in the square "belt" that, however, still carries a somewhat larger charge (over four atoms together). The electron-density distribution in $C_2Al_6^-$ is qualitatively similar to that in (structurally analogous) flat C_2Al_4, with a major concentration along the AlCCAl axis. The AIM calculations indicate critical points only for the axial C−Al bonding, hence ionic bonding between the "belt" and C_2.

A hydrocarbon-like, ethane-shaped C_2Al_6 structure has been investigated as well, in particular because the aluminum subsystem in this case would geometrically resemble an isolated Al_6 cluster (skewed rectangle bipyramid), thus offering a good match. The system is found, however, to relax into an aluminum "cup" made of 3-atom skewed "bottom" and 3-atom "rim" around the C_2 waist, with dicarbon protruding from it (Figure 3b). The symmetric C_2H_6-like structure (compressed along the C−C axis, Figure 3d) is a transition state between two equivalent "cup"-based geometries, only 0.3 eV higher in energy. This "end-on" isomer is 0.5 eV more stable than the "side-on" one, apparently due to a more efficient C−Al bonding, as reflected in a 0.06 Å longer C−C bond (Table 1).

The negative charge on the dicarbon is higher in this isomer (also relative to all other dicarbon-based systems) and concentrates on the atom with more Al neighbors (electron density donors). This carbon is the most negative atom for all systems studied in this work, which supports its formal hepta-coordination (to all other atoms in the cluster).

The AIM critical points, however, indicate tetra-bonded carbons, one to the atoms of the rim (in a strained configuration with the CCAl angles less than 80 °) and the other to the atoms of the bottom, with a reduced electron density in the C−C bond (Table 4). The (positive) Al atoms are charged more evenly than in the side-on isomer (Table 3). Both isomers have comparable, small dipole moments.

The higher stability of the end-on isomer is reflected in its significantly higher (by more than 1 eV) energies for ionization and triplet-excitation (the highest values among those for the species studied here). The electron affinity is, however, nearly the same as for the side-on isomer (Table 2).

The corresponding anion preserves the overall geometry of the neutral system, the most pronounced variations being somewhat longer C−Al and shorter Al−Al separations (Table

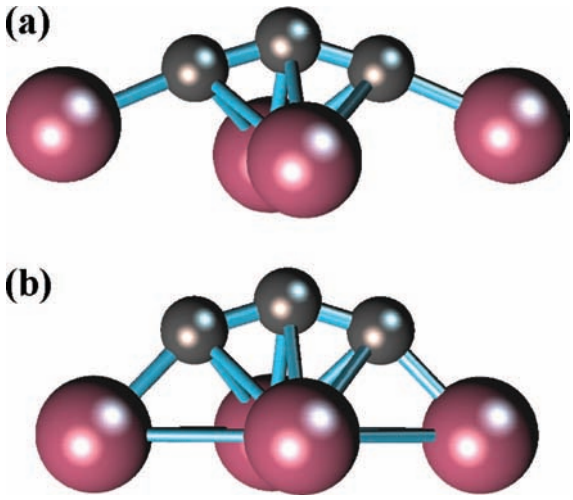

Figure 4. Optimized geometry of C_3Al_4 (a) and its anion (b).

1), oppositely to the other isomer. The adiabatic electron affinity is calculated as 1.24 eV, and the vertical electron-detachment energy is 1.33 eV. Both values are considerably lower than for the side-on isomer. The two isomers are less stable to dissociation than their neutral counterparts, with the reduction being stronger for the end-on isomer. It is worth noting that the joint binding energy of the two additional side Al atoms is about same (7 eV) as for the other side pair, which is different from the neutral systems.

In the anion, the extra negative charge goes completely to the aluminum cup, reducing its positive charge (Table 3). The charge distribution in the dicarbon remains almost unaffected upon charging the end-on C_2Al_6 isomer. This is completely different from the side-on isomer considered above.

DFT(PBE0) calculations qualitatively reproduce the shapes (and symmetries) of both (neutral) isomers, with the atom−atom distances deviating from the MP2 values within 0.05 Å for the side-on and by up to 0.2 Å (Al−Al) and 0.3 Å (side C−Al) for the end-on isomer. Unlike at the MP2 level, the isomers are predicted to be almost degenerate in energy, with the end-on one still being marginally more stable (by 0.02 eV). The DFT dissociation energies for both isomers are lower by about 2 eV (or 10%).

C_3Al_4. Formally adding another carbon to C_2Al_4 results in a C_{2v}-symmetric side-on structure with the C_3 arc ($\angle CCC = 147°$) attached to the slightly bent Al_4 rhombus (Figure 4). In particular, such a geometry is obtained when starting from either C_3H_4 (propyne)-like, that is, symmetric Al_2CCCAl_2 or C_3H_4 (propadiene)-like, that is, asymmetric $AlCCCAl_3$ structures. The C−C bond lengths are almost unchanged, and the C−Al separations slightly shorten (axial one) or stretch (side one) as compared to rhombic C_2Al_4 (Table 1). The C_3-Al_4 binding is 0.6 eV lower than for C_2-Al_4, apparently due to strain in bent C_3. This strain stretches Al_4 by 0.1 Å in the nearest-neighbor (nondiagonal) Al−Al distances relative to its unperturbed geometry.

By comparison, DFT(PBE0) calculations predict a less perturbed (more compact and flatter) Al_4 component. The Al−Al distances are 0.1−0.2 Å shorter, whereas the C−C and C−Al separations are the same as at the MP2 level within 0.03 Å, and the dissociation energy is about 2 eV (or 15%) smaller.

The C_3 molecule is, thus, too long to fit into the Al_4 frame; hence, it bends and protrudes sideways. The charges on the outer carbons are the same as in flat C_2Al_4, with the central carbon being only slightly negative. All aluminum atoms are evenly charged and are slightly more positive than in the dicarbon-based analogue. As a result of the nonflat geometry, C_3Al_4 has a dipole moment, although it is relatively small (Table 3).

The AIM calculations exhibit critical points only for the C−C and axial C−Al bonding, the bonding of carbons to the side aluminum atoms is thus ionic. The electron densities show a minor redistribution from the C−C to axial C−Al regions as compared to flat C_2Al_4 (Table 4).

The system is highly stable to ionization and triplet-excitation, whose energies are second only to those of side-on C_2Al_6 and significantly exceed (by more than 1 eV) those for analogous side-on C_2Al_4. The electron affinity is, however, the same as for this smaller counterpart (Table 2).

In the similarly shaped anion (Figure 4b), the aluminum rhombus becomes flat and shrinks (by up to 0.5 Å in the Al−Al distances), whereas the tricarbon geometry and C−Al distances remain almost unaffected (Table 1). The vertical electron-detachment energy is predicted to be 2.2 eV, and the adiabatic electron affinity of C_3Al_4 is 1.96 eV. In the anion, the extra charge is distributed over the aluminum frame (making it less positive), and an additional negative charge is transferred to it from the outer carbons (Table 3).The charge reduction on the aluminum atoms weakens their mutual (Coulomb) repulsion, which can explain the shrunken Al_4 unit.

C_3Al_6. The above mismatch of sizes between the carbon and aluminum components is removed when the latter one is extended by two atoms. The system becomes flat, with tricarbon symmetrically framed by aluminum atoms (Figure 5a). In particular, such a structure is produced by optimization from the C_3H_6(propene)-like geometry. Two flat CAl_3 units can be viewed to be connected together via a central C atom. The outer carbons show a planar tetra-coordinated bond-pattern. The Al−Al distances are considerably shorter (by around 0.5 Å) than in the smaller, (rhombic) C_2Al_4 analogue (Table 1). The binding is lower than in C_2Al_4, C_3Al_4 or C_2Al_6, both per atom and relative to separation into carbon and aluminum components.

At the DFT level, C_3 fits into the Al_6 frame a little less perfectly; the outer carbons slightly (and equally) protrude in the opposite directions from the plane (with the still linear tricarbon being thus at 5 ° to it), while all atom-atom distances being same within 0.01 Å. The flat geometry is a virtually nonexistent (0.003 eV higher in energy) saddle point between two equivalent equilibrium geometries.

Compared to C_3Al_4, the negative charges are higher on the outer carbons of C_3 and lower on the central carbon, with the tricarbon being more negative overall due to more Al donors of electron density (Table 3). The almost-neutral central carbon appears to have two double bonds to the outer C atoms that would thus have five bonds each, consistent with their high negative charges. Such an interpretation, questioning the formal planar hexa-coordination of the central atom, is supported by the electron-density distribution (Figure 5c) and by the AIM results below. All Al atoms in the frame are evenly positive, although with a lower charge per atom relative to C_3Al_4 (again due to the larger frame).

The AIM calculations predict critical electron densities for the axial C−Al bonding in C_3Al_6 at 18% of the values for the C−C bonds (Table 4), that is, the same ratio as in flat C_2Al_4 (and C_2Al_2). These densities for C_3Al_6 are slightly lower than in C_2Al_4. Each side C−Al bonding is equivalent to the axial one in terms of the critical electron density, thus confirming the largely ionic bonding between the outer carbons and aluminum atoms.

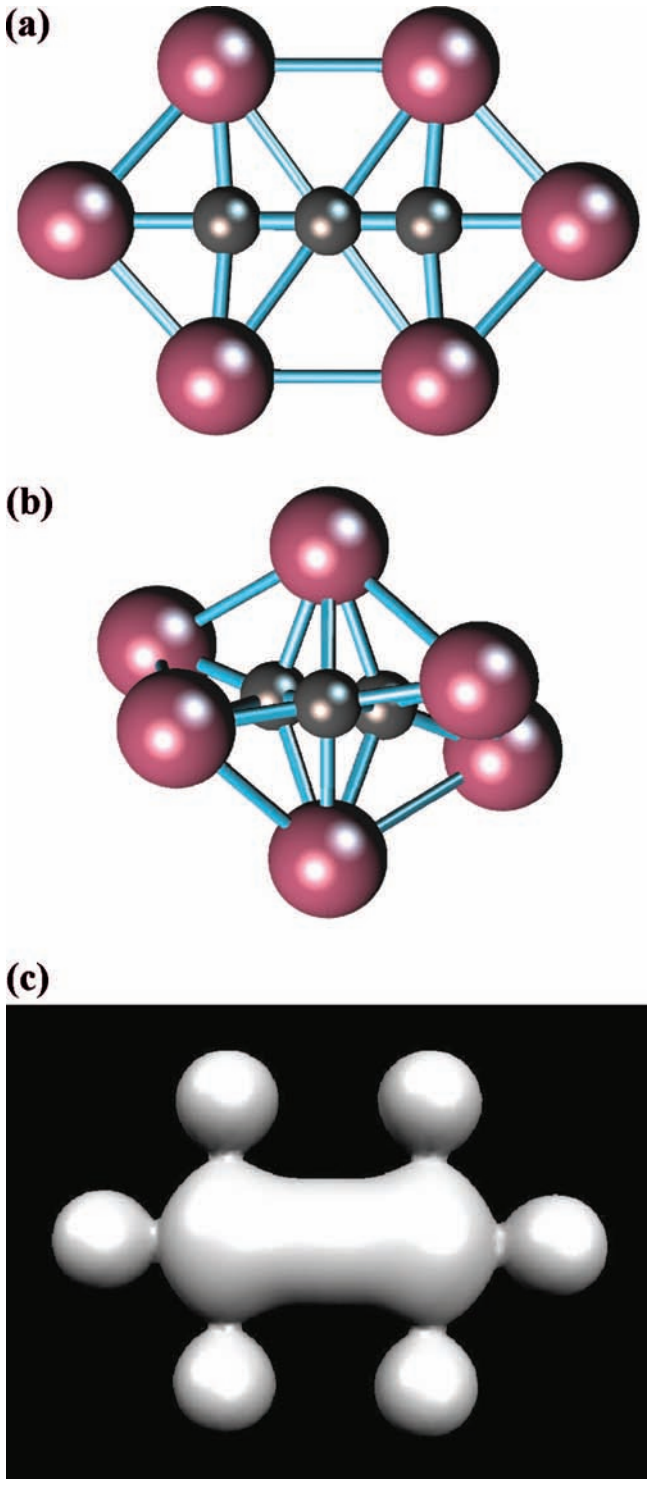

Figure 5. Optimized geometries of planar (a) and C_3-cycle-based C_3Al_6 (b) and calculated electron-density in the planar isomer (c).

Another isomer can be obtained when starting from the C_3H_6 (cyclopropane)-like geometry. The optimized structure has an isosceles-triangular C_3 core surrounded by Al atoms (Figure 5b), two under and above its plane and four around, also out of plane (equatorial). This isomer is only 0.1 eV lower in energy, with the strain in the carbon cycle (with longer C−C bonds) thus compensated by a more efficient C−Al bonding. The range of the C−Al separations is narrower, whereas the Al−Al separations are longer than in flat C_3Al_6 (Table 1). The negative charge on the C_3 cycle is higher than in the linear tricarbon in the flat isomer, and there is a small dipole moment (Table 3).

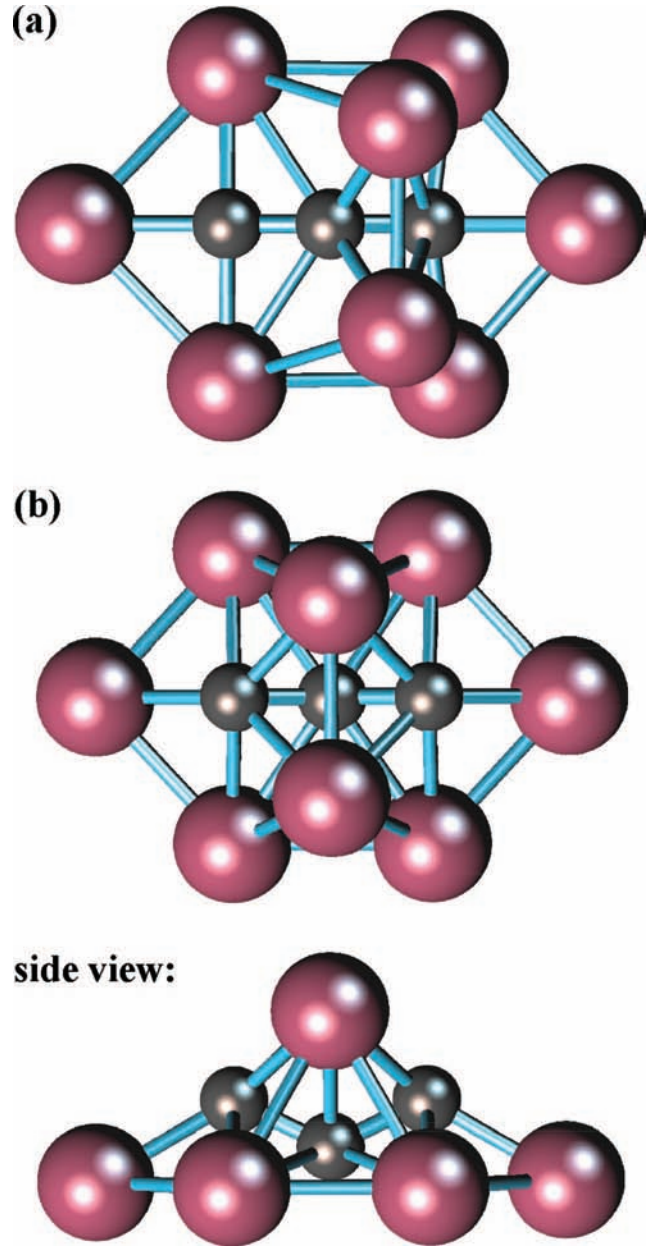

Figure 6. Optimized geometries of C_3Al_8 with convex (a) and concave C_3 (b).

In this isomer each carbon is formally hexa-coordinated (to both other C atoms, to two Al atoms above and under the C_3 plane, and to the two nearest other Al atoms). The AIM critical points indicate two carbons (at the shorter C−C distance) bonded to one of the above/under-plane Al and to one equatorial Al atoms. The remaining carbon (having longer bonds to the other C atoms) appears to also be bonded to both the above- and under-plane Al atoms as well as to two equatorial ones. This formally adds up to six bonds for this atom, including four (C−Al) with a strong ionic character. The critical electron densities are lower (especially in the C_3 cycle) than for the flat isomer (Table 4).

DFT(PBE0) calculations for this isomer reproduce all MP2 nearest-neighbor atom−atom distances within 0.1 Å. However, it is predicted to be significantly more stable (by 0.72 eV) than the other, (near-)flat isomer, contrary to the MP2 results. The dissociation energy is smaller by about 3 eV (15%) for both isomers.

TABLE 5: Vibrational Frequencies with Highest IR Intensities (in cm^{-1} and $D^2/Å^2$) of C_nAl_m and $C_nAl_m^-$

system		ν	I
C_2Al_2	linear	597	18.4
	T-shaped	725	3.76
$C_2Al_2^-$	T-shaped	629	8.3
C_2Al_4	flat	544, 590	8.75, 15.3
	side-on	573, 1674	8.47, 5.75
$C_2Al_4^-$	flat	622, 733	8.43, 70.2
C_2Al_6	end-on	494, 608, 675	3.16, 6.34, 5.63
	side-on	497, 591	2.89, 9.58
$C_2Al_6^-$	bipyramid	2 × 567, 682	2 × 11.1, 12.7
C_3Al_4		547, 1792	16.7, 11.6
$C_3Al_4^-$		361, 561, 746	4.53, 4.19, 4.35
C_3Al_6	flat	495, 605, 1848	6.86, 11.7, 35.2
	C_3-cycle	390, 505, 539	4.06, 6.10, 12.4
C_3Al_8	convex C_3	379, 478, 578, 1724	1.51, 4.72, 6.60, 1.44
	concave C_3	414, 476, 504, 1351	1.45, 4.20, 4.72, 4.20

The C_3-cycle-based isomer has higher ionization and triplet-excitation energies than the flat isomer, whereas the electron affinity is about the same for both isomers (Table 2). The flat isomer is the least stable to ionization of all the systems studied in this work. Both isomers have all the three energy parameters lower than those of C_3Al_4.

C_3Al_8. Adding two more Al atoms to C_3Al_6 perturbs its geometry, making it somewhat nonflat and making the tricarbon convex ($\angle CCC = 153°$), that is, angled toward the attached dimer. Both added atoms attach on the exposed side of the tricarbon, similar to the case of side-on C_2Al_6, although asymmetrically, closer to one end of C_3 (Figure 6a). In particular, such a structure of C_3Al_8 is obtained when starting from the C_3H_8 (propane)-like system. The C−C and C−Al separations somewhat stretch, and the Al−Al distances shorten relative to those in flat C_3Al_6 (Table 1).

Another, more symmetric isomer essentially preserves the flat Al_6 frame, while being 0.3 eV lower in energy. The tricarbon is pulled somewhat farther from the frame toward added Al_2 (as compared to the previous isomer) and is more strongly bent (to 128 °) but concave, angling away from the additional aluminum dimer that is centrally attached (Figure 6b). The C−C and axial C−Al separations are slightly longer, and the side C−Al and Al−Al distances and more uniform (Table 1).

At the DFT level, reoptimization of C_3Al_8 with convex C_3 relaxes it into the other isomer, although with the tricarbon less concave ($\angle CCC = 159$ °) and thus less protruding from the Al_6 frame than at the MP2 level. The C−C and axial C−Al distances are 0.1 Å shorter, whereas side C−Al and Al−Al are 0.2 and 0.1 Å longer, respectively.

The (MP2) binding energy of the additional Al_2 unit to the C_3Al_6 base is calculated to be 5.3−5.6 eV for both isomers (being slightly larger for the one with concave tricarbon). The total binding energy per Al atom is about the same as for C_3Al_6, similar to the analogous C_2Al_4/C_2Al_6 case (Table 1).

Compared to flat C_3Al_6, the central carbon is donated a considerable electron density from the additional aluminum atoms, and in the convex-C_3 isomer the negative charge on the outer carbons is slightly redistributed toward the atom with more Al neighbors (Table 3). The out-of-plane Al_2 unit leads to noticeable dipole moments in the systems, with a higher value for the concave-C_3 isomer.

In the concave isomer, each outer C atom is formally hexa-coordinated (including Al atoms in the nearer half of the frame and in added Al_2). AIM calculations exhibit all these C−Al interactions as having critical points, the electron densities associated with the added Al atoms being comparable to those between the outer C and side Al atoms. Hence, each outer C atom appears to have six bonds (including five strongly ionic C−Al ones). The central carbon is again bonded to the outer carbons only, as in flat C_3Al_6. Both C−C and C−Al critical electron densities are somewhat lower than in flat C_3Al_6 (Table 4).

Addition of Al_2 to flat C_3Al_6 somewhat increases all vertical electronic perturbation energies in the system (Table 2). These energy values are uniformly slightly lower for the isomer with concave C_3.

Conclusions

A series of alumino-carbon clusters, C_nAl_m ($n = 2-3$, $m = 2-8$) have been computationally investigated at a MP2 level of theory with correlation consistent basis sets augmented on carbon. All systems beyond C_2Al_2 are structurally different from their stoichiometric hydrocarbon counterparts (with equal number of hydrogen atoms) due to ionic bonding of the Al atoms to the carbon molecular centers. AIM calculations also indicate a weak covalent C−Al bonding, especially for Al atoms located along the di- and tricarbon axes. The C_2Al_2 core is still present in larger dicarbon-based species, C_2Al_4 and C_2Al_6, with other aluminum atoms attached sideways. In C_nAl_m, the carbon molecule can be submerged into the aluminum subsystem (as, e.g., in $C_2Al_6^-$ and C_3-cycle-based C_3Al_6), lie on its surface (as in C_3Al_4), or be incorporated into it (in C_2Al_6).

Stable isomers of C_2Al_4 and C_3Al_6 are predicted to have flat geometries, with the dicarbon and tricarbon symmetrically framed by aluminum atoms. These systems exhibit unusual planar tetra-coordination of carbon. High negative charges (up to about −2e) on the C atoms can facilitate their hyper-coordination, for instance, with five nearest-neighboring atoms in C_2Al_6 and six in C_3Al_8. It is further promoted in the anions, such as $C_2Al_6^-$ with its hexa-coordinated carbons. One of the C atoms in the end-on isomer of C_2Al_6 is even hepta-coordinated. The AIM calculations, however, undermine hypervalence of carbon in these species. Only in some systems, such as C_3Al_6 and C_3Al_8, some carbon atoms appear, in terms of critical points, to have six bonds including those (C−Al) with strong ionic character.

Both planarity and hyper-coordination support a qualitative similarity between C_nB_m and the alumino-carbon clusters, possible in view of analogous valence electron configurations of the Al and B atoms. The related issue of aromaticity is beyond the scope of the present work.

Auxiliary DFT (PBE0) calculations at least qualitatively reproduce the predicted cluster geometries (and symmetries). Deviations include the opposite order in energy of two C_3Al_6 isomers, the absence of the C_3Al_8 isomer with convex tricarbon, and the lower dissociation energies for $m > 2$ (with the difference increasing with the cluster size).

The extra electron in some of the associated anionic species leads to a significant change of the cluster shape, from a moderate variation in $C_3Al_4^-$ (with shrinking Al_4 unit) to a considerable alteration in $C_2Al_6^-$ (with C_2 acquiring a square Al_4 belt and thus sinking into Al_6). These geometry changes are reversible upon neutralization of the anion (via electron-detachment) and could perhaps be considered for a possible use in molecular devices controlled by electric current at nanoscale.

Binding energies of the pairs of aluminum atoms subsequently added to dicarbon in the C_2Al_n series vary significantly in the neutrals (from 10 eV for axial bonds to 5 eV for side bonds) but are approximately equal in the anions (7 eV). In the C_3Al_n

series, the binding energies of subsequent Al pairs are more uniform, at 6−7 eV. This indicates, in particular, that the considered systems may not yet have a completed solvation shell of the aluminum atoms around the carbon molecular centers.

All the studied carbon−aluminum clusters exhibit a significant stability toward ionization (with the predicted IE values in excess of 7 eV) and moderate electron attachment (EA under 1.5 eV). They also have closed-shell electronic structures with appreciable singlet−triplet gaps (in excess of 2 eV in most cases). This may provide a sufficient chemical stability of such species, especially C_2Al_6 and C_3Al_4. To facilitate experimental detection of C_nAl_m, their calculated vibrational frequencies with the highest IR intensities are listed in Table 5.

Acknowledgment. Calculations have been carried out on the high-performance computing facilities of the University of Ontario Institute of Technology (UOIT) Faculty of Science and of the Sharcnet (Ontario network), and the author is grateful to their supporting staff. The Natural Sciences and Engineering Research Council (NSERC) of Canada is acknowledged for financial support (Discovery grant).

References and Notes

(1) Kiran, B.; Li, X.; Zhai, H.-J.; Wang, L.-S *J. Chem. Phys.* **2006**, *125*, 133204.

(2) Zubarev, D. Y.; Boldyrev, A. I.; Li, X.; Zhai, H.-J.; Wang, L.-S *J. Phys. Chem. A* **2007**, *111*, 1648.

(3) Naumkin, F. *Phys. Chem. Chem. Phys.* **2006**, *8*, 2539.

(4) Boldyrev, A. I.; Simons, J.; Li, X.; Wang, L.-S. *J. Am. Chem. Soc.* **1999**, *121*, 10193.

(5) Cannon, N. A.; Boldyrev, A. I.; Li, X.; Wang, L. S. *J. Chem. Phys.* **2000**, *113*, 2671.

(6) Li, X.; Wang, L. S.; Cannon, N. A.; Boldyrev, A. I *J. Chem. Phys.* **2002**, *116*, 1330.

(7) Boldyrev, A. I.; Simons, J.; Li, X.; Chen, W.; Wang, L.-S. *J. Chem. Phys.* **1999**, *110*, 8980.

(8) Exner, K.; Schleyer, P. V. *Science* **2000**, *290*, 1937.

(9) Zubarev, D. Y.; Boldyrev, A. I. *J. Chem. Phys.* **2005**, *122*, 144322.

(10) Li, X.; Wang, L.-S.; Boldyrev, A. I.; Simons, J. *J. Am. Chem. Soc.* **1999**, *121*, 6033.

(11) (a) Dunning, T. H., Jr. *J. Chem. Phys.* **1989**, *90*, 1007. (b) Woon, D. E.; Dunning, T. H., Jr. *J. Chem. Phys.* **1993**, *98*, 1358.

(12) Aprà, E., Windus, T. L., Straatsma, T. P., Bylaska, E. J., de Jong, W., et al, NWChem, a Computational Chemistry Package for Parallel Computers, v 4.7; Pacific Northwest National Laboratory: Richland, Washington, 2005; available at http://www.emsl.pnl.gov/docs/nwchem/.

(13) NIST Chemistry WebBook. NIST Standard Reference Database Number 69, June 2005 Release. http://webbook.nist.gov/chemistry/.

(14) Schultz, N. E.; Staszewska, G.; Staszewski, P.; Truhlar, D. J. *J. Phys. Chem. B* **2004**, *108*, 4850.

(15) Brazier, C. R. *J. Chem. Phys.* **1993**, *98*, 2790.

(16) Gutsev, G. L.; Jena, P.; Bartlett, R. J. *J. Chem. Phys.* **1999**, *110*, 2928.

(17) Bader, R. F. W. *Atoms in Molecules: A Quantum Theory*; Oxford University Press: Oxford, 1990.

(18) Ryzhkov, A.; Antipin, A. *ViewMol3D* 4.34, a 3D OpenGL viewer for molecular structures; available at http://redandr.tripod.com/vm3/.

(19) Flükiger, P.; Lüthi, H. P.; Portmann, S.; Weber, J. *MOLEKEL* 4.3; Swiss Center for Scientific Computing CSCS: Manno, Switzerland, 2000; available at http://www.cscs.ch/molekel/.

JP711230X